A Feedback Based Modification of the NDVI to Minimize Canopy Background and Atmospheric Noise

Hui Qing Liu and Alfredo Huete

Abstract—**The Normalized Difference Vegetation Index (NDVI) equation has a simple, open loop structure (no feedback), which renders it susceptible to large sources of error and uncertainty over variable atmospheric and canopy background conditions. In this study, a systems analysis approach is used to examine noise sources in existing vegetation indices (VI's) and to develop a stable, modified NDVI (MNDVI) equation. The MNDVI, a closed-loop version of the NDVI, was constructed by adding 1) a soil and atmospheric noise feedback loop, and 2) an atmospheric noise compensation forward loop. The coefficients developed for the MNDVI are physically-based and are empirically related to the expected range of atmospheric and background "boundary" conditions. The MNDVI can be used with data uncorrected for atmosphere, as well as with Rayleigh corrected and atmospherically corrected data. In the field observational and simulated data sets tested here, the MNDVI was found to considerably reduce noise for any complex soil and atmospheric situation. The resulting uncertainty, expressed as vegetation equivalent noise, was ±0.11 leaf area index (LAI) units, which was 7 times less than encountered with the NDVI (±0.8 LAI). These results indicate that the MNDVI may be satisfactory in meeting the need for accurate, long term vegetation measurements for the Earth Observing System (EOS) program.**

I. Introduction

VEGETATION indexes (VI) are radiometric measures of vegetation used to assess the temporal and spatial variations of many plant biophysical parameters, such as leaf area index (LAI), absorbed photosynthetically active radiation (APAR), and %green cover. They have been successfully used to measure vegetation in agricultural areas, local and regional scale landscapes, and global scale biomes [1]–[3]. The physical basis of the VI "signal" is attributed to the absorption of incident red light by plant chlorophyll and scattering of incident near-infrared (NIR) radiation by plant leaves. Thus, each band is an indicator of the amount of vegetation, however, signal contributions from nonvegetation components such as canopy background and atmosphere render individual band relationships with biophysical plant parameters very unstable. The ratio of reflected radiance from these two bands normalizes a significant amount of illumination and topographic variation, and forms a more stable indicator of the amount and vigor of green vegetation [4]. The difference of these two bands divided by their sum forms the functionally equivalent, normalized difference vegetation index [5]

$$\mathrm{NDVI} = \frac{\rho_{\mathrm{Nir}} - \rho_{\mathrm{Red}}}{\rho_{\mathrm{Nir}} + \rho_{\mathrm{Red}}} \tag{1}$$

which, over terrestrial surfaces, is constrained between 0 and 1 when reflectances, ρ, rather than radiances, are used. However, the NDVI has been shown to be very sensitive to canopy background and atmospheric influences [6], [7]. In general, dark or wet soil backgrounds result in higher NDVI values relative to brighter soils for a constant vegetation amount, and high atmospheric aerosol contents (low visibilities) produce lower NDVI signals relative to clear, low aerosol atmospheres. Soil background noise tends to decrease with increasing vegetation cover while the influence of the atmosphere on the NDVI becomes greater over higher levels of vegetation. Furthermore, soil background and atmospheric noise in the NDVI are not independent, but interact in a complex manner since the atmosphere also alters the soil background signal and vice-versa.

In a sensitivity analysis with the SAIL model, [8] found atmospheric-induced noise in the NDVI to be more pronounced over canopies with darker soil backgrounds and soil-induced noise in the NDVI was lower with increases in atmospheric aerosol contents. Thus, increases in atmospheric noise lowered the NDVI signal, but minimized soil noise in the NDVI. These individual and 'coupled' influences on the NDVI result in an error and uncertainty in the ability of the NDVI to accurately predict biophysical vegetation amounts and associated, inter- and intra-annual changes.

Several atmospheric- and soil-correcting variants of the NDVI have recently been proposed, including the Soil Adjusted Vegetation Index (SAVI) [9] and Modified Soil Adjusted Vegetation Index (MSAVI) [10], the Atmospherically Resistant Vegetation Index (ARVI) [11], and the Soil Adjusted and Atmospherically Resistant Vegetation Index (SARVI) [11]. In observational and SAIL model sensitivity studies, all of the NDVI variant vegetation indexes (SAVI, ARVI, and SARVI) were found to outperform the NDVI in decreasing soil noise and/or atmospheric noise relative to the NDVI signal [8], [12]. The SARVI was able to predict LAI to within ±0.36 LAI throughout a large range of atmospheric, soil and vegetation conditions, in contrast to a level of noise of ±0.8 LAI in the NDVI.

Manuscript received March 18, 1994. This work was supported in part by MODIS under contract NAS5-31364.

The authors are with the Department of Soil and Water Science, University of Arizona, Tucson, AZ 85721 USA.

IEEE Log Number 9407902.

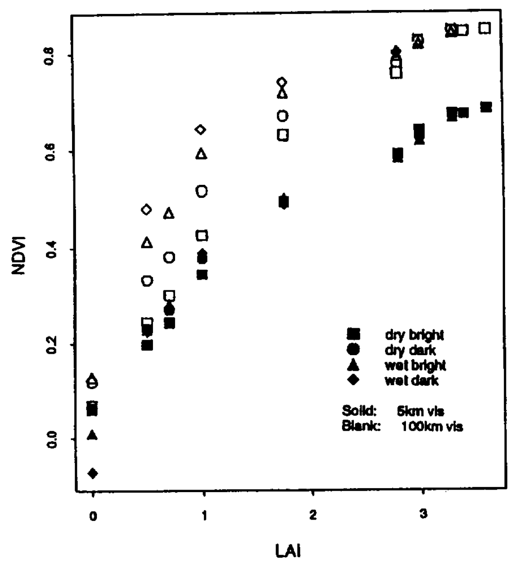

Fig. 1. NDVI values as a function of LAI for the experimental cotton data set with varying soil backgrounds and atmospheric simulated conditions.

Although the SARVI was found to markedly minimize soil background and atmospheric influences, relative to the NDVI, they were not both reduced in a systematic, predictable manner. This was due to the failure of the SARVI equation to consider combined or "coupled," interactive effects of soil and atmosphere. In this paper, a systems based, feedback approach is used to minimize both independent and interactive atmospheric and soil background influences on the VI signal under total, partial and no atmospheric correction scenarios. We similarly examined the structure of the NDVI, SAVI, MSAVI, ARVI and SARVI equations for instability and noise sources.

II. Data Description

Three sets of data were used in this paper. Field observational cotton (*Gossypivm hirsutrm L.* var DPL-70) canopy data with four soil background types under dry and wet conditions were measured using a Barnes "multimodular radiometer" (MMR) at various levels of vegetation cover (0–100% cover; 0–3.6 LAI) [6]. Similarly, field-based observational corn (*Zea mays L.*) canopy data, with four kinds of dry and wet soil backgrounds were measured with an Exotech Model 100 at vegetation LAI's from 0 to 4.2 [13]. The last data set, generated using the SAIL canopy radiative transfer model [14], represented a simulated cedar canopy with LAI's from 0 to 3 and with six kinds of soil background. In all three canopy data sets, bare soil reflectance ranged from 0.10 to 0.40 in the near-infrared. Atmosphere simulations were applied to these data sets with Mid-Latitude Summer and Rural Aerosol Models from Lowtran 7 [15]. Two sets of atmosphere simulated data were produced: 1) an aerosol and Rayleigh atmosphere with visibilities from 5 km to 100 km and 2) a Rayleigh corrected atmosphere with a similar range in aerosol contents. Over the range of surface reflectances utilized here, the relationship between surface reflectance and top of the atmospheric radiances were found to be linear with negligible error [16], [17].

III. Feedback Approach

In order to construct a stable soil and atmospheric, self-correcting vegetation index, one can use a "systems method" to analyze not only individual effects but also combination effects of all variables affecting the NDVI. A good vegetation index equation should be a closed-loop system with negative feedback and compensation terms for soil and atmospheric noise. A feedback system is not only stable but superior in many respects to systems without feedback by providing higher quality output values [18]. In this section, the unstable behavior of the NDVI is analyzed and a stable vegetation index or modified NDVI (MNDVI) is formulated.

A. Noise in NDVI

The NDVI (1) is a nonlinear operator of two bands (red and NIR): This is an open-loop system that lacks any feedback

$$X \longrightarrow \boxed{\frac{\rho_{nir} - \rho_{red}}{\rho_{nir} + \rho_{red}}} \longrightarrow \mathrm{NDVI}$$

Block Diagram 1. NDVI.

mechanism to compensate for variations in scattered and absorbed energy from the atmospheric medium and/or soil background. "X" is the mixture input signal from the surface containing vegetation, some soil, atmosphere and other noises, which strongly appear in the NDVI through the operator. Fig. 1 shows the dynamic behavior of the NDVI over a wide range of soil brightness, atmosphere visibility and ground LAI's using the observational cotton data. The unstable nature of the NDVI may be diagrammed as

Soil brightness $\uparrow \longrightarrow$ NDVI $\downarrow$
Atmospheric visibility $\downarrow \longrightarrow$ NDVI $\downarrow$

and

Atmospheric visibility $\downarrow \longrightarrow$ Soil noise $\downarrow$
Ground LAI $\uparrow \longrightarrow$ Soil noise $\downarrow$
Ground LAI $\uparrow \longrightarrow$ Atmospheric noise $\uparrow$.

The NDVI has an inverse tendency to soil brightness, and the same tendency with atmospheric visibility. Soil noise and atmospheric noise interact with each other and vary with amount of vegetation cover.

B. Modification of NDVI (MNDVI)

In the systems analysis method, the NDVI is stabilized by adding two noise correction loops: 1) an NDVI noise (soil and atmosphere noise) feedback loop, H_1, that introduces a part of the output MNDVI_0 (block diagram 2) to override initial noise input and 2) a noise compensation forward loop, H_2,

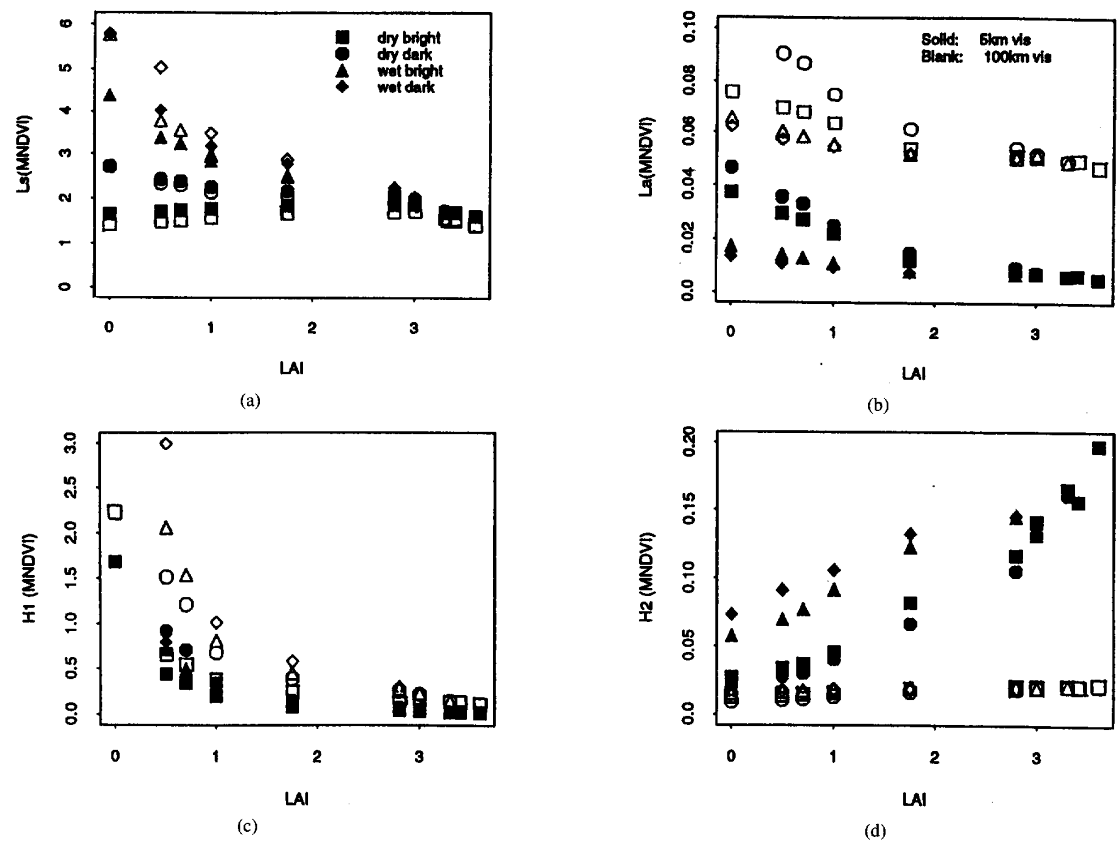

Fig. 2. Soil and atmospheric (A, B) feedback components, and H_1 feedback (C) and H_2 feed-forward (D) loops of the MNDVI as a function of LAI for the experimental cotton data set.

to compensate for the noise that the feedback loop could not overcome, such that

Soil brightnesss	$\downarrow\longrightarrow$ NDVI $\uparrow\longrightarrow H_1 \longrightarrow$ $\mathrm{MNDVI}_0 \downarrow\longrightarrow$ MNDVI $\downarrow$.
Atmospheric visibility	$\downarrow\longrightarrow$ NDVI $\downarrow\longrightarrow H_1 \longrightarrow$ $\mathrm{MNDVI}_0 \uparrow\longrightarrow$ MNDVI $\uparrow$.

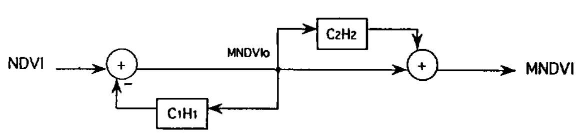

Block Diagram 2. MNDVI

MNDVI is the output of the system, the NDVI is the input of the system. The structure of the system (block diagram 2) becomes:

$$\mathrm{MNDVI} = \frac{\mathrm{NDVI}}{1 + C_1 H_1}(1 + C_2 H_2) = \mathrm{MNDVI}_0(1 + C_2 H_2) \tag{2a}$$

where

$$\mathrm{MNDVI}_0 = \frac{\mathrm{NDVI}}{1 + C_1 H_1}. \tag{2b}$$

Ideally, H_1 is a function of all soil and atmospheric noise in the NDVI. If the NDVI has no noise, then H_1 should be zero and when the NDVI has very high noise, H_1 should have maximum response. MNDVI_0 is a feedback version of the NDVI with H_1 designed so that the NDVI becomes self-correcting for soil and/or atmospheric influences. Any noise not accounted for in the feedback loop is then considered in H_2, which thus becomes a function of the remaining noise in MNDVI_0. If MNDVI_0 has successfully corrected soil and atmospheric noise, then H_2 should be zero. In order to control the amplitude of H_1 and H_2, two coefficients, C_1 and C_2 are used in the system.

In order for MNDVI_0 to fully correct for soil and atmospheric noise, H_1 must have the following relation with NDVI:

$$\mathrm{MNDVI}_0 = \mathrm{NDVI} - \triangle\mathrm{NDVI}, \tag{3a}$$

where $\triangle$NDVI is the noise in NDVI, and

$$\mathrm{MNDVI}_0 = \mathrm{NDVI} - H_1 \mathrm{MNDVI}_0, \tag{3b}$$

such that

$$H_1 = \frac{\triangle\mathrm{NDVI}}{(\mathrm{NDVI} - \triangle\mathrm{NDVI})} = \frac{\triangle\mathrm{NDVI}}{\mathrm{NDVI}_{\mathrm{true}}} \tag{3c}$$

where $\mathrm{NDVI}_{\mathrm{true}}$ is the ideal NDVI (not including any noise).

Equation (3c) shows that H_1 is proportional to the variation of NDVI due to soil brightness and atmosphere visibility, and inversely proportional to the $\mathrm{NDVI}_{\mathrm{true}}$. Thus, H_1 should primarily increase with a decrease of ground vegetation cover (more soil, hence more feedback needed), and become lower with increasing vegetation in order to maintain the vegetation signal. H_1 should also increase with a decrease in soil brightness and increase with greater atmospheric visibilities, since under clearer atmospheric conditions, soil noise also becomes stronger and more feedback is required.

Generally, it is not possible for H_1 to simultaneously remove multiple sources of noise. If H_1 is primarily designed for soil noise feedback, then a second noise compensation function H_2 is used to remove atmosphere noise from MNDVI_0. Then H_2 should increase with a decrease in atmospheric visibility and an increase of vegetation. H_2 should compensate for atmospheric noise without introducing soil noise.

Based on these points and the optical characteristics of the soil-canopy-atmosphere, H_1 and H_2 were designed as

$$H_1 = L_s L_a L_v = \frac{C_{11}\rho_{\mathrm{Red}} - \rho_{\mathrm{Blue}} + C_{12}}{\rho^2_{\mathrm{Nir}} - \rho^2_{\mathrm{Red}}} \tag{4a}$$

where

$$L_s = \frac{1}{\rho_{\mathrm{Nir}} + \rho_{\mathrm{Red}}} \tag{4b}$$

$$L_a = C_{11}\rho_{\mathrm{Red}} - \rho_{\mathrm{Blue}} + C_{12} \tag{4c}$$

$$L_v = \frac{1}{\rho_{\mathrm{Nir}} - \rho_{\mathrm{Red}}} \tag{4d}$$

and

$$H_2 = \frac{1}{L_a} = \frac{1}{C_{11}\rho_{\mathrm{Red}} - \rho_{\mathrm{Blue}} + C_{12}} \tag{4e}$$

The three components of H_1 (L_s, L_a, L_v) are further described

1) L_s is the feedback component to account for soil brightness variations in the NDVI. In Fig. 2(a), L_s is higher for dark and wet soil backgrounds, demonstrating the higher feedback required, since dark canopy backgrounds raise NDVI values. L_s also decreases with increasing LAI due to the lower soil signal.
2) L_a is an atmospheric noise feedback term, to account for variations in soil noise under different atmospheric conditions [Fig. 2(b)]. L_a decreases at lower atmospheric visibilities, making H_1 smaller and NDVI higher, since less soil feedback correction is required with the dampened soil signals found under turbid atmospheres. The coefficients, C_{11} and C_{12}, determine how the blue band is utilized to adjust the red band for atmosphere following the approach of Kaufman and Tanré [11]. These coefficients are a function of the range of atmosphere and soil brightness conditions expected and are not dependent on the characteristics of the vegetation canopy.

The constant, C_{12} is a higher atmospheric boundary condition coefficient, providing enough soil noise feedback without an atmosphere (infinite visibility) and also avoiding too much feedback under the lowest atmospheric visibility (5 km visibility). C_{11} is the lower atmospheric boundary condition coefficient, providing proper atmospheric feedback for the lowest atmospheric visibility. These coefficients were set at $C_{11} = 0.55$ and $C_{12} = 0.12$, based on: 1) atmospheric visibilities ranging from 5 km to 100 km and; 2) canopy background reflectances ranging from 0.10 (very dark) to 0.40 (very bright) in the near-infrared. Fig. 2(b), diagrams the lower feedback, L_a, with lower atmospheric visibility and higher vegetation LAI.

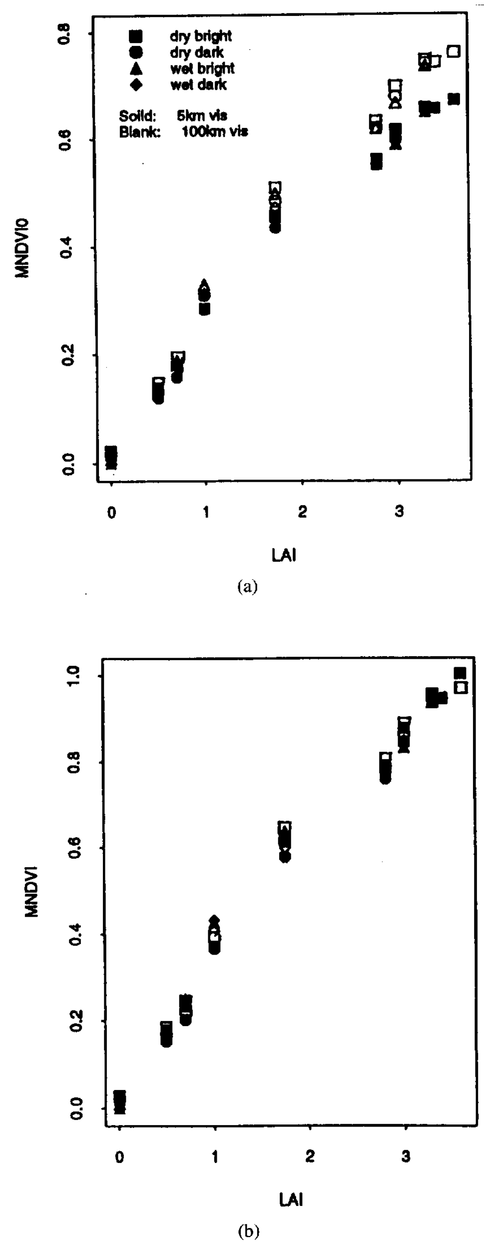

Fig. 3. MNDVI_0 (a) and MNDVI (b) values as a function of LAI for the experimental cotton data set with varying soil backgrounds and atmospheric simulated conditions.

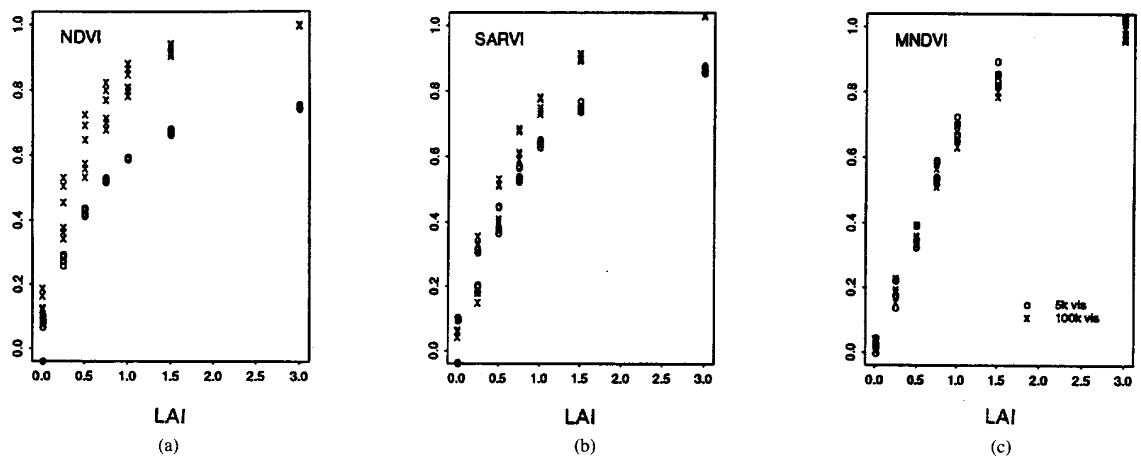

Fig. 4. NDVI (a), SARVI (b), and MNDVI (c) values as a function of LAI for the simulated SAIL-cedar data set with varying soil backgrounds and atmospheric simulated conditions.

3) L_v is for ground vegetation cover feedback, which makes soil noise feedback decrease with an increase of vegetation amount. This not only maintains the vegetation signal, but also results in a more linear vegetation signal which produces great sensitivity over a wider range of vegetation amounts.

H_1 now has the desired behavior of decreasing with increasing soil brightness, increasing vegetation LAI, and lower atmospheric visibilities [Fig. 2(c)]. H_2, on the other hand, is inversely proportional to atmospheric feedback, L_a. It is primarily used to compensate for atmospheric noise, as well as to restore the vegetation signal in MNDVI_0. It is sensitive to decreases in atmospheric visibility and increases in ground vegetation cover. In Fig. 2(d), H_2 has the desired effect of increasing strongly with atmospheric turbidity (lower visibility) and higher amounts of vegetation.

In summary, 1) as the amount of vegetation on the ground increases, H_1 decreases and H_2 increases; 2) as soil brightness increases, H_1 decreases and; 3) as atmospheric visibility decreases, H_1 decreases and H_2 increases. It is important to note that the H_1 and H_2 feedback terms are not empirical functions of particular data sets, but instead, are empirically related to the boundary conditions of expected atmospheric and soil brightness conditions. The physical basis for the atmospheric and canopy background adjustments are reported in [9], [11].

C. MNDVI with Total, Partial and No Atmospheric Correction

An ideal VI would not only be invariant to a large range of atmospheric conditions, but should also be somewhat invariant to the degree and uncertainties expected in atmospheric correction algorithms. Thus, the MNDVI should work well with: 1) nonatmospherically corrected data, 2) partial atmospheric corrected data (Rayleigh scattering, gas absorption), and 3) total atmosphere correction (remove aerosol, gas, and Rayleigh). A partial or complete atmospheric correction will increase the NDVI and increase soil noise, relative to nonatmospherically corrected data. The amplitude of the feedback terms, H_1 and H_2, in the MNDVI can be adjusted for these different conditions with the loading coefficients, C_1 and C_2.

In general (2),

$$\mathrm{MNDVI} = \frac{\mathrm{NDVI}}{(1 + C_1 H_1)}(1 + C_2 H_2) \tag{5}$$

where H_1 is (4a) and H_2 is (4e), C_1 and C_2 are

1) No atmos-correction:	C_1 and C_2 = 0.001
2) Partial atmos-correction:	C_1 = 0.6,and C_2 = 0.03
3) Total atmos-correction:	C_1 = 0.6, and C_2 = 0.03

If the data is Rayleigh corrected (cases 2 and 3), then the feedback, H_1, increases too much and C_1 is lowered accordingly. C_2 is higher under Rayleigh corrected data since the lowered C_1 results in too little atmospheric feedback.

D. MNDVI Test Results

Two parameters, Vegetation Equivalent Noise (VEN) and relative error ($\Delta_r(\%)$) were used to estimate the quality of the VI's [12]. VEN is defined as

$$\mathrm{VEN} = \frac{\mathrm{VI}_p - \mathrm{VI}}{S(\mathrm{LAI})} \tag{6}$$

where VI is the "true" or mean vegetation index value at any given LAI; VI_p is the atmospheric- and soil-perturbed response; and S(LAI) is the slope of the VI$\sim$LAI curve at a specific LAI. The absolute error, Δ_a, is simply $\mathrm{VI}_p-\mathrm{VI}$, and the relative error is defined as

$$\Delta_r(\%) = \frac{100(\mathrm{VI}_p - \mathrm{VI})}{\mathrm{VI} - \mathrm{VI}_s} \tag{7}$$

where VI_s is the bare soil VI response (lower boundary condition for the VI dynamic range).

Using the cotton data, Fig. 3(a) shows that the MNDVI_0 has fairly good soil correction, but only a partial atmospheric correction, particularly at the higher LAI's. On the other hand, MNDVI [Fig. 3(b)] has achieved both soil and atmospheric correction due to the additional compensation from H_2. We also tested the MNDVI on two separate independent data sets, namely the SAIL-simulated cedar canopy and the observational corn canopy data. The cotton and corn canopies had completely different canopy architectures, planophile and erectophile, while the cedar canopy had a uniform distribution of leaf orientations. As shown in Fig. 4 the MNDVI successfully normalized the extreme range of atmospheric and soil conditions in the simulated, SAIL-cedar data, in comparison with the NDVI and SARVI. The averaged vegetation equivalent noise (VEN) over the entire range of LAI's for all three canopy data sets are shown in Fig. 5 for all VI's. The level of uncertainty in the MNDVI ($\pm$ 0.11 LAI units) was the same for all three canopy data sets. This was three times lower than the SARVI ($\pm$ 0.36) and nearly seven times less than the uncertainty in the NDVI ($\pm$ 0.8 LAI) in all three (cotton, cedar and corn) data sets.

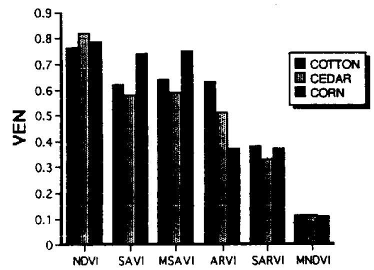

Fig. 5. Vegetation equivalent noise values (LAI) for the various VI's using the experimental cotton and corn data sets and simulated SAIL-cedar data with varying soil and atmospheric conditions.

IV. Noise Analysis of Vegetation Indexes

In this section, the noise inherent in the NDVI variant equations, and the apparent relationships between the NDVI and the variants are analyzed.

A. SAVI

The SAVI was introduced to minimize the soil brightness influence in the NDVI [9]:

$$\mathrm{SAVI} = (1 + C)\frac{\rho_{\mathrm{Nir}} - \rho_{\mathrm{Red}}}{\rho_{\mathrm{Nir}} + \rho_{\mathrm{Red}} + C} \qquad C = 0.5 \tag{8a}$$

where C, a soil-vegetation interaction term, provides compensation for soil noise, Huete [9] reported $C = 0.5$ to work well over a wide range of soil and vegetation amounts in ground-based data without an atmosphere. However, the SAVI remains unstable with respect to atmospheric variations and soil-induced noise may re-appear in data sets of varying atmospheres. The SAVI may be described in terms of the NDVI by

$$\mathrm{SAVI} = (1 + C)\frac{\mathrm{NDVI}}{1 + H_{1(\mathrm{SAVI})}} \tag{8b}$$

$$H_{1(\mathrm{SAVI})} = \frac{C}{\rho_{\mathrm{Nir}} + \rho_{\mathrm{Red}}}. \tag{8c}$$

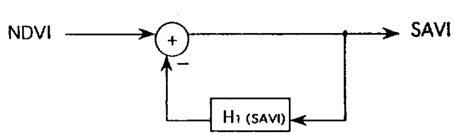

Block Diagram 3. SAVI

This is a closed-loop system with NDVI as input of the system and $H_{1(\mathrm{SAVI})}$ providing feedback from the NDVI. Fig. 6(a) shows $H_{1(\mathrm{SAVI})}$ to have a strong negative feedback with darker soils at low LAI's. However, the soil feedback does not approach zero at higher LAI's where there is little soil signal. This reduces the vegetation signal at high levels of vegetation cover. $H_{1(\mathrm{SAVI})}$ also has a slight positive feedback with atmosphere at high ground vegetation covers. This makes the SAVI have more atmospheric noise than NDVI at high ground vegetation covers.

B. MSAVI

Reference [10] introduced the Modified Soil Adjusted Vegetation Index (MSAVI) to further minimize soil influences by using a variable soil brightness correction factor, C, to replace the constant soil correction, 0.5 in the SAVI,

$$\mathrm{MSAVI} = (1 + C_{\mathrm{MSAVI}})\frac{\rho_{\mathrm{Nir}} - \rho_{\mathrm{Red}}}{\rho_{\mathrm{Nir}} + \rho_{\mathrm{Red}} + C_{\mathrm{MSAVI}}}. \tag{9a}$$

Two versions of the MSAVI were proposed:

MSAVI_1 has

$$C_{\mathrm{MSAVI1}} = 1 - 2\gamma \mathrm{NDVI}(\rho_{\mathrm{nir}} - \gamma\rho_{\mathrm{red}}) \tag{9b}$$

with $\gamma = 1.06$;

MSAVI_2 is with

$$\begin{aligned} C_{\mathrm{MSAVI2}} &= 1 - \mathrm{MSAVI}_2 \\ &= 1 - 1/2\Big\{2\rho_{\mathrm{nir}} + 1) \\ &\qquad - \sqrt{[(2\rho_{\mathrm{nir}} + 1)^2 - 8(\rho_{\mathrm{nir}} - \rho_{\mathrm{red}})]}\Big\}. \end{aligned} \tag{9c}$$

The MSAVI may be described in terms of the NDVI by

$$\mathrm{MSAVI} = \frac{\mathrm{NDVI}}{(1 + H_{1(\mathrm{MSAVI})})}(1 + H_{2(\mathrm{MSAVI})}) \tag{9d}$$

where

$$H_{1(\mathrm{MSAVI})} = C_{\mathrm{MSAVI}}/(\rho_{\mathrm{nir}} + \rho_{\mathrm{red}}), \text{ and} \tag{9e}$$

$$H_{2(\mathrm{MSAVI})} = C_{\mathrm{MSAVI}}. \tag{9f}$$

Fig. 6(b) and (c) shows H_1 and H_2 in MSAVI_1 (H_1 and H_2 in MSAVI_1 are very similar to ones in MSAVI_2). $H_{1(\mathrm{MSAVI})}$ has negative soil feedback, and positive atmospheric feedback. $H_{1(\mathrm{MSAVI})}$ approaches zero at high LAI's, but is somewhat high at intermediate LAI levels. This is in contrast to the desired H_1 behavior seen in the MNDVI [Fig. 2(c)], whereby H_1 provides negative atmospheric feedback. As in the SAVI, this results in higher levels of atmospheric noise. The purpose of $H_{2(\mathrm{MSAVI})}$ is to provide compensation for too much negative soil feedback and positive atmospheric feedback from

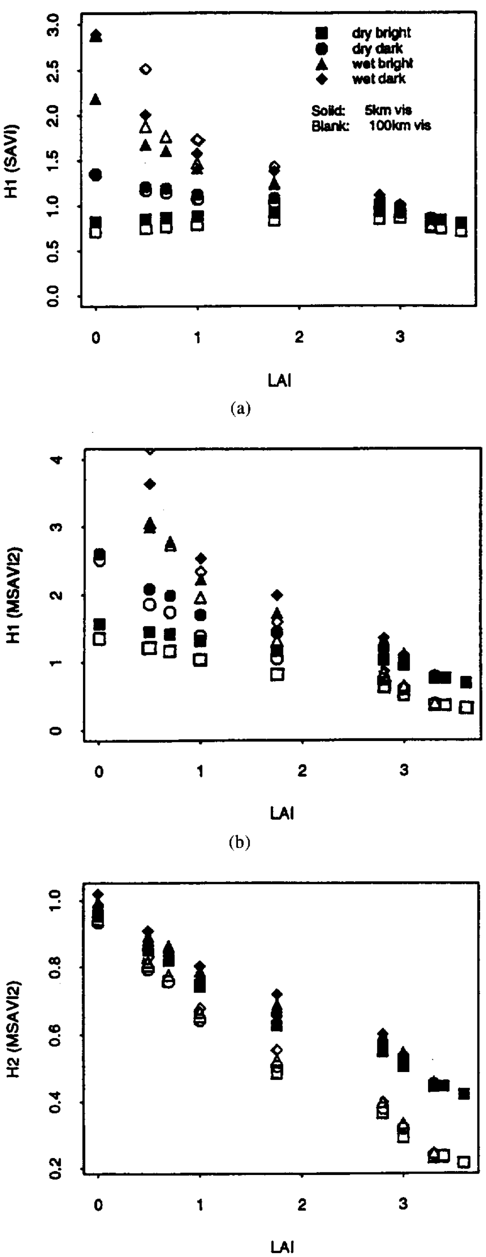

Fig. 6. H_1 feedback behavior for the ASVI (a) and MSAVI (b) and H_2feed-forward for the MSAVI (c) as a function of LAI for the experimental cotton data set with varying soil backgrounds and atmospheric simulated conditions.

$H_{1(\mathrm{MSAVI})}$. Overall, the SAVI and MSAVI are fairly identical in correction for soil and atmospheric noise (Fig. 5), although the MSAVI required two loops to remove only the soil noise.

C. ARVI

The ARVI was introduced to decrease atmospheric aerosol influences in Rayleigh corrected data, by adding a blue band to the NDVI equation [11]

$$\mathrm{ARVI} = \frac{\rho^*_{\mathrm{Nir}} - \rho^*_{\mathrm{rb}}}{\rho^*_{\mathrm{Nir}} + \rho^*_{\mathrm{rb}}} \tag{10a}$$

where

$$\rho^*_{\mathrm{rb}} = \rho^*_{\mathrm{Red}} - \gamma(\rho^*_{\mathrm{Blue}} - \rho^*_{\mathrm{Red}}) \tag{10b}$$

(ρ^* is apparent reflectance with Rayleigh correction).

By utilizing the difference in the radiance between the blue and the red channels, one corrects the radiance in the red channel for atmospheric effects reducing atmospheric noise in the NDVI. Reference [8] found the ARVI to significantly reduce atmospheric-induced noise but at the expense of increasing the soil noise component. The ARVI may be described in terms of the NDVI by

$$\mathrm{ARVI} = \frac{\mathrm{NDVI}}{1 + H_{1(\mathrm{ARVI})}}(1 + H_{2(\mathrm{ARVI})}) \tag{10c}$$

$$H_{1(\mathrm{ARVI})} = \frac{\gamma(\rho^*_{\mathrm{Red}} - \rho^*_{\mathrm{Blue}})}{\rho^*_{\mathrm{Nir}} + \rho^*_{\mathrm{Red}}} \tag{10d}$$

$$H_{2(\mathrm{ARVI})} = \frac{\gamma(\rho^*_{\mathrm{Blue}} - \rho^*_{\mathrm{Red}})}{\rho^*_{\mathrm{Nir}} - \rho^*_{\mathrm{Red}}}. \tag{10e}$$

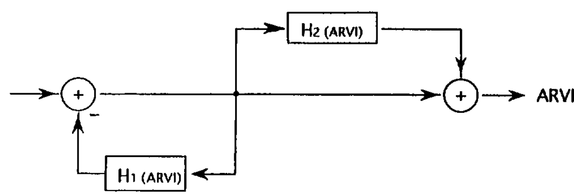

Block Diagram 4. ARVI

This is also a two loop system with H_1 as the feedback loop and H_2 as the feed-forward loop. $H_{1(\mathrm{ARVI})}$ has the desired behavior of strong negative feedback with atmosphere, but it has positive, rather than negative, feedback with soil brightness [Fig. 7(a)]. This makes ARVI decrease in atmospheric noise and increase in soil noise relative to the NDVI. $H_{2(\mathrm{ARVI})}$ [Fig. 7(b)] is a new feed-forward loop of the three bands (blue, red and NIR) which is not so sensitive to atomsphere over the range of vegetation LAI's compared with H_1, and produces more soil noise when LAI <2. $H_{2(\mathrm{ARVI})}$ does not help the ARVI in removing atmospheric noise, but brings in significant additional soil noise.

D. SARVI

By combining the soil adjustment factor, C, in the SAVI with the blue band and γ term in the ARVI, one derives the SARVI which attempts to correct for both soil and atmospheric effects

$$\mathrm{SARVI} = (1 + C)\frac{\rho^*_{\mathrm{Nir}} - \rho^*_{\mathrm{rb}}}{\rho^*_{\mathrm{Nir}} + \rho^*_{\mathrm{rb}} + C} \qquad C = 0.5. \tag{11a}$$

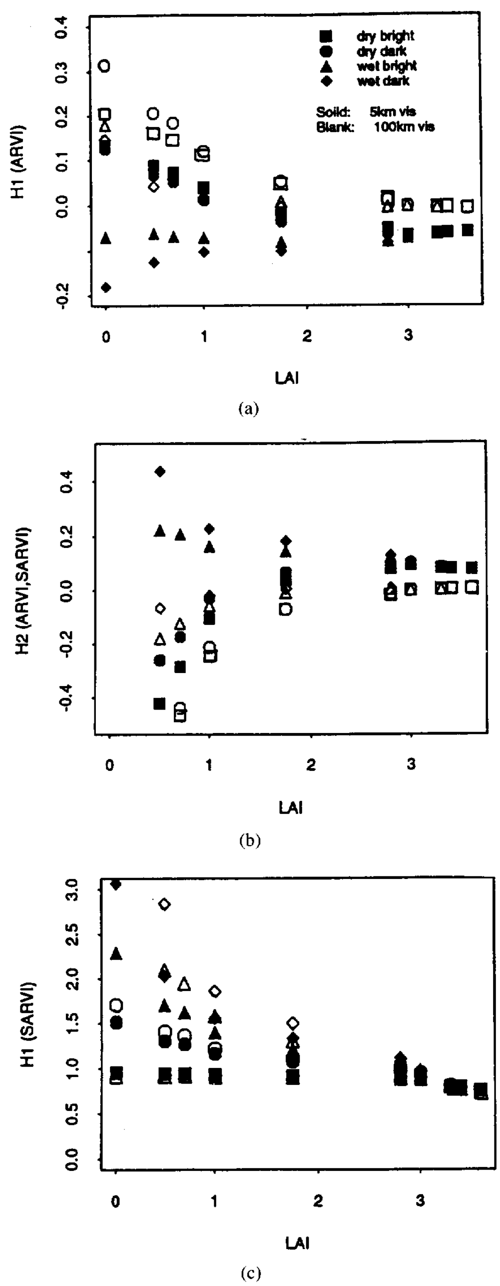

Fig. 7. H_1 feedback behavior for the ARVI (a) and SARVI (c) and H_2 feedforward for the ARVI and SARVI (b) as a function of LAI for the experimental cotton data set with varying soil backgrounds and atmospheric simulated conditions.

The SARVI equation may be described in terms of the NDVI by

$$\mathrm{SARVI} = (1 + C)\frac{\mathrm{NDVI}}{1 + H_{1(\mathrm{SARVI})}}(1 + H_{2(\mathrm{SARVI})}), \quad (11b)$$

which follows the same block diagram as with the ARVI (block diagram 4), making $H_{2(\mathrm{SARVI})}$ the same as $H_{2(\mathrm{ARVI})}$ [Fig. 7(b)]. The $H_{1(\mathrm{SARVI})}$ feedback function, however, differs from that of the ARVI as a result of the constant, $C = 0.5$

$$H_{1(\mathrm{SARVI})} = \frac{\gamma(\rho^*_{\mathrm{Red}} - \rho^*_{\mathrm{Blue}}) + C}{\rho^*_{\mathrm{Nir}} + \rho^*_{\mathrm{Red}}}. \quad (11c)$$

The addition of the soil-adjusted constant, C, results in $H_{1(\mathrm{SARVI})}$ having a much stronger, negative soil brightness feedback [Fig. 7(c)]. But this reduces atmospheric feedback strongly. Also, the soil feedback is too high when LAI >1, resulting in a loss in the VI signal. As with the ARVI, $H_{2(\mathrm{SARVI})}$ helps to reduce atmospheric noise, but brings in additional soil noise.

In summary, the SAVI equation has good soil negative feedback, but lacks atmospheric negative feedback. The ARVI equation has effective atmospheric negative feedback, but also has positive soil noise feedback. The SARVI equation has only a partial, atmospheric and soil noise negative feedback.

V. Conclusion

A systems based modification of the Normalized Difference Vegetation Index (NDVI), utilizing feedback loops, was made to account for both soil background and atmospheric sources of noise and error. Soil and atmospheric influences in the NDVI as well as in the NDVI variants were examined. The NDVI had the highest levels of noise and error, whereas the NDVI variant equations (SAVI, MSAVI, ARVI, SARVI) partially removed soil and/or atmospheric noise to varying degrees. Because soil and atmospheric effects are interactive and vary with vegetation cover, they produce a very complex effect on vegetation indexes. By decreasing one noise the others increased, hence the need for a systems approach with appropriate soil and atmospheric feedback mechanisms.

The MNDVI, based on a closed-loop system, overcame the disadvantages of the SARVI and other VI's. The MNDVI can correct for soil effects over a wide range of atmospheric conditions from 5 km to infinity visibility. The MNDVI had the lowest vegetation equivalent noise (VEN) ($\pm$0.11 LAI units) in comparison with the NDVI and NDVI variants ($\pm$0.36 to $\pm$0.8 LAI units) for both experimental and simulated data sets.

The feedback approach in the MNDVI effectively minimized the atmospheric and soil 'bias' present in the NDVI and other VI's. Vegetation sensitivity was also enhanced and MNDVI-plant biophysical relationships were more linear, thus reducing the saturation problem commonly found in similar relationships involving the NDVI. Although three different canopy data sets were tested here, a greater range of canopy and atmospheric conditions need to be tested under field, aircraft, satellite, and simulation conditions. A wide range of atmospheric visibilities were tested here (5 km to 100 km), however, other atmospheric aerosol models, such as the tropical model, need testing. The removal of "bias" and enhancement of the vegetation signal are crucial to the development of global-based VI's, which require vegetation measures to be invariant too external influences.

The global application and compositing of the MNDVI will require further analyses with respect to the influences of sub-pixel clouds and shadow, topography, and sun-target-sensor geometries. In the EOS era, a bidirectional reflectance distribution function (BRDF) algorithm will be implemented, facilitating solar and view angle corrections to the VI. More detailed topographic data, as well as advanced cloud and shadow masks, will also be available. Thus, spatial and temporal variations in atmospheric aerosol concentrations and canopy backgrounds (soil color, roughness, moisture, and surface litter) remain as the highest sources of uncertainty in VI products. An operational atmospheric correction of EOS data for land surface studies are also planned, however, it may not be possible to implement a globally consistent scheme (e.g., dark-object subtraction method). This presents justification to maintain some resistance to atmospheric influences in the VI itself, as the quality of the correction may vary greatly and there is a need to maintain some degree of integrity and continuity in the VI global data base.

ACKNOWLEDGMENT

The authors thank K. Batchily, J. Epiphanio, and H. Y. Liu for assistance with the model and simulations.

REFERENCES

[1] R. B. Myneni, B. D. Ganapol and G. Asrar, "Remote sensing of vegetation canopy photosynthetic and stomatal conductance efficiencies," *Remote Sensing Environ.*, vol. 42, pp. 217–238, 1992.

[2] P. J. Sellers, S. Los, C. J. Tucker, C. O. Justice, D. A. Dazlich *et al.*, "A global $1^\circ * 1^\circ$ NDVI data set for climate studies. Part 2—The adjustment of the NDVI and generation of global fields of terrestrial biophysical parameters," *Int. J. Remote Sensing*, in press.

[3] S. D. Prince, "A model of regional primary production for use with coarse resolution satellite data," *Int. J. Remote Sensing*, vol. 12, no. 6, pp. 1313–1330, 1991.

[4] C. J. Tucker, "Red and photographic infrared linear combinations for monitoring vegetation," *Remote Sensing Environ.*, vol. 8, pp. 127–150, 1979.

[5] D. W. Deering, "Rangeland reflectance characteristics measured by aircraft and spacecraft sensors," Ph.D. dissertation, Texas A&M Univ., College Station, 1978, p. 338.

[6] A. R. Huete, R. D. Jackson, and D. F. Post, "Spectral response of a plant canopy with different Soil backgrounds," *Remote Sensing Environ.*, vol. 17, pp. 37–53, 1985.

[7] P. N. Slater and R. D. Jackson, "Atmospheric effect on radiation reflected from soil and vegetation as measured by orbiting sensors using various scanning directions," *Appl. Opt.*, vol. 21, pp. 3923–3931, 1982.

[8] A. R. Huete and H. Liu, "An error and sensitivity analysis of the atmospheric and soil correcting variants of the NDVI for MODIS-EOS," *IEEE Trans. Geosci. Remote Sensing*, vol. 32, pp. 897–905, July 1994.

[9] A. R. Huete, "A soil-adjusted vegetation index (SAVI)," *Remote Sensing Environ.*, vol. 25, pp. 295–309, 1988.

[10] J. Qi and A. R. Huete, "Modified soil adjusted vegetation index (MSAVI)," *Remote Sensing Environ.*, vol. 48, pp. 119–126, 1994.

[11] J. Kaufman and D. Tanré, "Atmospherically resistant vegetation index (ARVI) for EOS-MODIS," *IEEE Trans. Geosci. Remote Sensing*, vol. 30, 261–267, Mar. 1992.

[12] A. R. Huete, C. Justice, and H. Liu, "Development of vegetation and soil indices for MODIS-EOS," *Remote Sensing Environ.*, vol. 48, pp. 1–13, 1994.

[13] W. Bausch, "Soil background effects on reflectance-based crop coefficients for corn," *Remote Sensing Environ.*, vol. 46, pp. 1–10, 1993.

[14] W. Verhoef, "Light scattering by leaf layers with application to canopy reflectance modeling: The SAIL model," *Remote Sensing Environ.*, vol. 16, pp. 125–141, 1984.

[15] F. X. Kneizys, E. P. Shettle, L. W. Abreu, J. H. Chetwynd, G. P. Anderson *et al.*, "User Guide to LOWTRAN 7," Rep. AFGL-TR-88-0177, AFRCL, Bedford, MA, p. 137, 1988.

[16] S. Moran and R. D. Jackson, "Obtaining surface reflectance factors from atmospheric and view angle corrected SPOT-1 HRV data," *Remote Sensing Environ.*, vol. 32, pp. 203–214, 1990.

[17] S. Moran and R. D. Jackson, "Evaluation of simplified procedure for retrieval of land surface reflectance factors from satellite sensor output," *Remote Sensing Environ.*, vol. 41, pp. 169–184, 1992.

[18] J. Choma, Jr., *Electrical Networks Theory and Analysis.* New York: Wiley, 1985.

Hui Qing Liu, photograph and biography not available at time of publication.

Alfredo Huete, photograph and biography not available at time of publication.